IV International Conference on Particle-based Methods – Fundamentals and Applications
PARTICLES 2015
E. Oñate, M. Bischoff, D.R.J. Owen, P. Wriggers & T. Zohdi (Eds)

APPLICATION OF THE LATTICE-BOLTZMANN METHOD FOR MODELING ALL-VANADIUM REDOX FLOW BATTERIES

Dario Maggiolo[1], Francesco Picano[1] Andrea Marion[1] and Massimo Guarneri[1]

[1] Department of Industrial Engineering, University of Padova
dario.maggiolo@unipd.it, www.unipd.it

Key words: Redox Flow Battery, Lattice-Boltzmann Method, Porous Media, Mixing

Abstract. All-Vanadium Redox Flow Batteries (VRFBs) represent a promising technology as a way to store energy because of their high energy efficiency, long cycle life, independently tunable power/energy size, and lack of contamination from cross-mixing of electrolytes.However, in order to improve VRFBs performance, some conceptual and technological issues are still open. In particular, a properly designed geometry of flow channels and porous medium, which guarantees a uniform distribution of the reacting species all along the electrode, is still under investigation.The ideal configuration aims to minimize the drag maximising the mixing. This will guarantee an increase of the performance and of the overall efficiency. In the present work a Lattice Boltzmann tri-dimensional multi-relaxation-time model (LBM) has been used to better understand the dependence of mass and momentum transports on the porosity and carbon fiber preferential orientation. The LBM has been coupled with a Lagrangian particle tracking algorithm in order to investigate the dispersion mechanisms induced by the porous medium on the species flowing in a typical VRFB. Results show that the drag measured by the permeability K is considerably reduced when the medium fibers are preferentially oriented along the streamwise direction, as expected. The fiber orientation also affects the species mixing that needs to be enhanced to optimize the VRFB performance. Surprisingly, the medium with fibers preferentially oriented along the streamwise direction, among all the considered medium, shows also the highest transversal dispersion rate characterized by super-diffusive behavior. In light of these results, this anisotropic medium appears to be optimal to enhance VRFBs performances by reducing the drag and enhancing the mixing.

1 INTRODUCTION

During the last years, VRFBs have been perceived as one of the most promising technologies to improve electrochemical energy storage. In comparison with other batteries, VRFBs are characterized by higher energy efficiency, longer cycle life and more flexible

power/energy sizing [1]. Even though the VRFB technology is well-known since the late 1980's, it is only during recent years that the scientific community has focused on improving VRFBs performance [1, 3]. A cell of a VRFB cell is composed by two porous media electrodes of carbon fibers. The inner surfaces of the porous media act as active site where electrochemical reduction and oxidation reactions of the Vanadium electrolytes occur. The reduction reaction at one electrode extracts electrons and ions from one electrolyte, while the oxidation at the other electrode recombines them into the other electrolyte. Ions may migrate from anode to cathode through a ion exchange membrane which separates the two half-cells. Both half-cells are fed by external storage tanks which pump freshen electrolyte solutions in the porous media electrode to keep on the reactions. The peak performance of VRFB is limited by a too slow electrolyte transport in the electrodes [1].

The fluid dynamic optimization of the porous medium which acts both as electrochemical active surface and as a mixing layer of chemical species in VRFBs is one of the main technological issues to be dealt [2].

Actually, the slow diffusion process of Vanadium species in water often represents a bottleneck for the peak performance of VRFBs.Specifically, the mass diffusion coefficients of the Vanadium species in water, $D \sim 10^{-10}\, m^2\, s^{-1}$, are about 10000 smaller than the water kinematic viscosity, $\nu = \mu/\rho \sim 10^{-6}\, m^2\, s^{-1}$ indicating that the mass diffusion is 10000 times slower than the momentum transport. The fibers constituting the porous medium enhance the effective mass transport perturbing the flow trajectories at microscales.A proper designed geometry of the porous medium may enhance this effective mass transport and minimize the drag improving and optimizing the VRFB performances. This is the topic of the present study.

While the influence of porous medium porosity on the flow drag has been largely studied [4], the impact of its microscopic design on mixing/transport mechanisms and drag is still not well assessed [4, 5].

In order to clarify this issue, several simulations varying the preferential orientation of fibers at different porosity and Reynolds number have been carried out by means of a Lattice-Boltzmann-based model coupled with a Lagrangian particle tracking algorithm. The aim of the present paper is to clarify how the nematic properties of the porous medium affects the mass and momentum transport mechanisms in order to design optimal porous media with low drag and high effective mass diffusion. The minimization of drag reduces the required pump power, while the maximization of the mixing improves the uniformity of reacting species all along the porous medium, resulting in enhanced performances of VRFBs. We will show that porous media constituted by fibers preferentially oriented along the flow direction exhibit smaller drag and higher effective diffusion.

2 NUMERICAL METHOD

In recent years the Lattice-Boltzmann Method (LBM) proved to be a good solution in solving Navier-Stokes Equations, allowing easy implementation and algorithm parallelization, especially in presence of complex geometries [6]. In the present work a

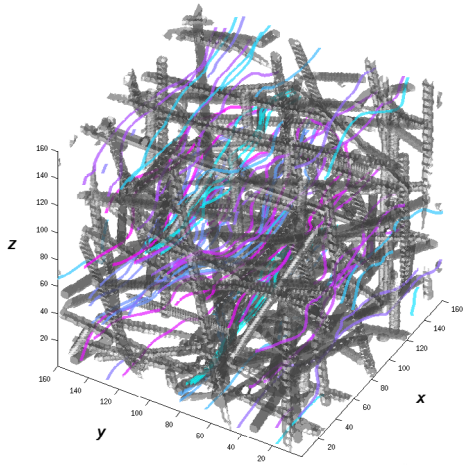

Figure 1: Tri-periodic cubic domain with particle trajectories for the isotropic case with poroisty $\varepsilon = 0.9$. The domain size is 160^3 and the flow is driven by a pressure gradient along x.

three-dimensional multi-relaxation time Lattice-Boltzmann model has been developed to simulate the fluid flow inside a fiber-composed porous medium. The model has been successfully validated against theoretical solutions of the Volume Averaged Navier-Stokes Equations [7]. The multi-relaxation-time lattice Boltzmann equation reads as follows:

$$f_i(\mathbf{x} + \mathbf{c}_i, t + 1) - f_i(\mathbf{x}, t) = -\mathbf{M}^{-1}\mathbf{S}\big(m_i(\mathbf{x}, t) - m_i^e(\mathbf{x}, t)\big) \ , \tag{1}$$

where $f_i(\mathbf{x}, t)$, is the distribution function $\mathbf{x}$ at the time t along the i-th lattice direction, $m_i(\mathbf{x}, t)$ and $m_i^e(\mathbf{x}, t)$ are the moment and the equilibrium moment obtained by the Gram-Schmidt orthogonalization procedure; $\mathbf{c}$ is the discrete speed vector, S is the collisional matrix and M the transformation matrix [8].

The typical porosity used in VRFB, $\varepsilon = 0.7 \div 0.9$, is considered in a triperiodic box, see Fig.(1). The flow is driven along the x direction by a mean pressure gradient DP/Dx which imposes the Reynolds number Re$= Ud_f\rho/\mu = 0.1 \div 1.0$ with U the bulk velocity, d_f the fiber diameter, ρ the fluid density and μ the dynamic viscosity. The side of the periodic box is discretized by 160 computational cells, while the fiber diameter d_f corresponds to 6 cells. Three different porous medium orientations have been considered: an isotropic medium, a medium preferentially oriented along the streamwise direction and a medium preferentially oriented along the transverse direction. The medium is considered preferentially oriented along the streamwise or transverse direction when all the angles formed by the axes of the fibers and the x axis are lower or higher than $\pi/4$, respectively.

Since the diffusion coefficients of the Vanadium species in water are very small and the main aim is to characterize the effective diffusion induced by the porous medium micro-structure, the mass transport properties are evaluated following non-Brownian tracer

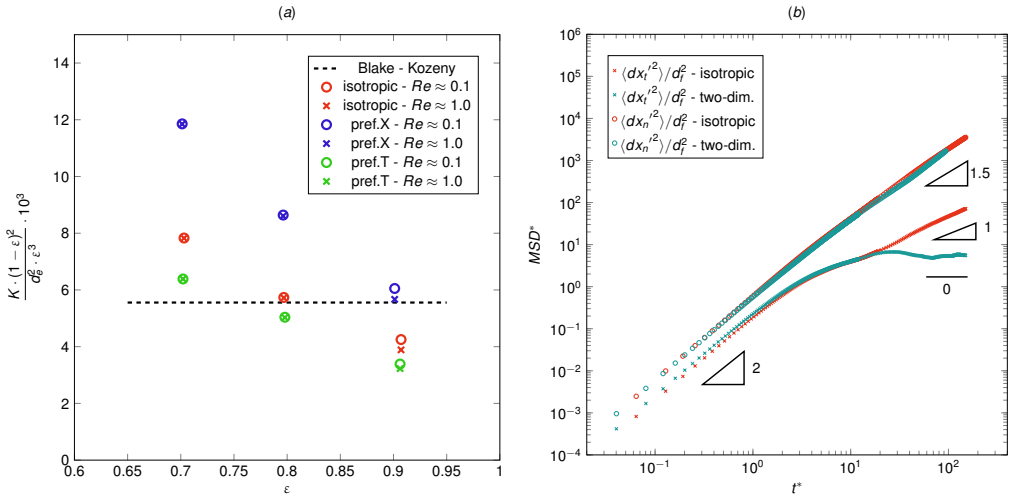

Figure 2: (a) Non-dimensional permeability with varying the porosity, the fiber orientation and the Reynolds number. The Blake-Kozeny equation is depicted by a black-dashed line. (b) Non-dimensional Mean Square Displacement plotted against the characteristic observation time for the isotropic case (red line) and the two-dimensional case (turquoise line).

particles injected in the fluid. The LBM stationary flow field has been used as input of the Lagrangian Particle tracking algorithm, see Fig.(1), and Lagrangian statistics of ten thousand particles have been analyzed in order to extract the effective diffusion coefficients in the porous media. Particles are randomly injected in the fluid phase and their trajectories are stored in time. All the observables shown in the following analysis have been normalized using the bulk velocity U and the fiber diameter d_f.

3 RESULTS

In the theoretical framework of flows in porous media, the Darcy's law is often used to describe the ability of the fluid to flow through the medium. It considers the bulk velocity U, which is the mean of the fluid velocity in the whole volume, and relates it to the pressure gradient by means of the permeability K [4]:

$$K = \varepsilon U \mu \cdot \left(-\frac{DP}{Dx} \right)^{-1} . \tag{2}$$

Fig.(2) shows the values of non-dimensional permeability K with varying the porosity and the porous medium orientation (left panel). The values of K of the isotropic medium are consistent with experimental values available in literature [4] and can be approximated using the Blake-Kozeny equation: $K/d_e^2 = \varepsilon^3/[180\,(1-\varepsilon^2)]$. It is strictly valid for packed beds of spheres, but can be used for cylindrical-shaped fibers using the characteristic length $d_e = 3/2 \cdot d_f$, see [4]. A decreasing behavior with increasing the porosity ε has been reported also in experimental investigations, see e.g. [4]. The values of permeability of the medium preferentially oriented along the transverse direction are

similar to the isotropic ones and well captured by Blake-Kozeny equation. On the contrary, the medium preferentially oriented along the streamwise direction presents much higher values of permeability, which correspond to lower flow drag inside the porous medium.Moreover, Fig.(2) clearly shows that the influence of finite Reynolds number on permeability is negligible in the present investigation range.

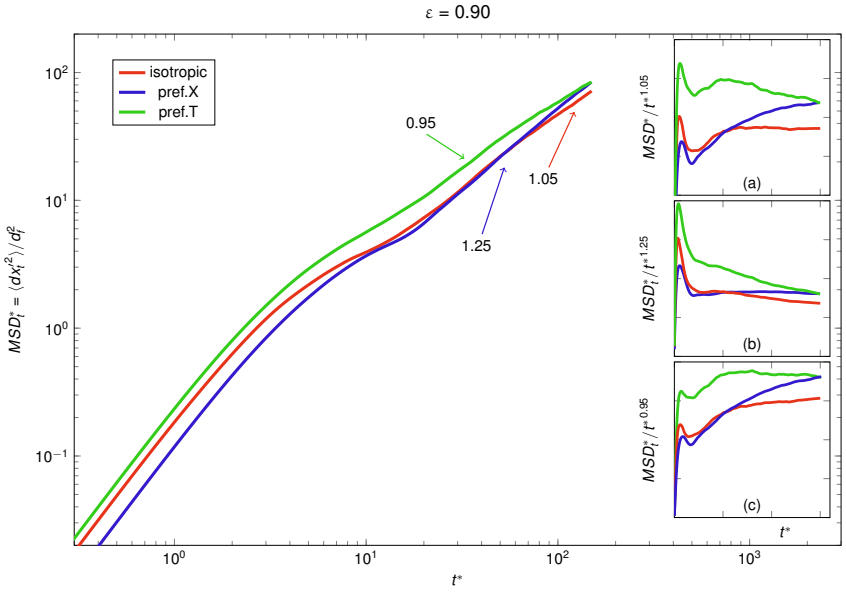

Figure 3: Non-dimensional Mean Square Displacement for three different orientation and $\varepsilon = 0.9$. Insets (a), (b) and (c): Non-dimensional mean square displacement normalized by $t^{1.05}$, $t^{1.25}$ and $t^{0.95}$, respectively.

The right panel of Fig.(2) instead shows the values of the non-dimensional mean square displacement MSD^* along the streamwise and transverse directions with increasing the observation time t^*. Two cases are shown: the isotropic medium and a medium fully oriented along one transversal direction y. This last case corresponds to a 2D porous medium in the (x, z) plane formed by circular solid being completely homogenous in the other direction. The non-dimensional values MSD^* and t^* are defined as follows:

$$MSD^*_{n,t} \equiv \frac{\langle dx'^{\,2}_{n,t} \rangle}{d_f^2} \tag{3}$$

$$t^* \equiv t \cdot \frac{U}{df} \tag{4}$$

where $dx'_{n,t} = x_{n,t} - \langle x_{n,t} \rangle$ is the fluctuation of the displacement $x_{n,t}$ along the streamwise (subscript n) or transverse (subscript t) direction and $\langle\rangle$ indicates the averaging ensemble operator. The MSD^* is initially proportional to t^{*2} for all the considered cases, denoted by a slope 2 in the log-log plot of Fig.(2). This is an expected behavior until the particle

motion is still correlated. After a characteristic time $t^* \approx 10$, the behavior of the MSD^* along the streamwise direction changes as $MSD^* \propto t^{*\alpha}$ with $\alpha = 1.5$ for both cases. This exponent corresponds to a super-diffusive behavior and has been reported also in the recent paper of [5]. The super-diffusion process denotes an incredibly fast anomalous diffusion which has been found in biological and peculiar physical systems. While no significant differences are found in the dispersion along the streamwise direction between the two cases, the behavior dramatically changes in the transversal direction where the isotropic case exhibits an unitary exponent denoting a standard diffusion, while the 2D case shows a constant MSD^*, i.e. $\alpha = 0$. This behavior is not strange since the particle trajectories live in a 2D steady case where chaotic mixing cannot be observed. In other words, it indicates that the particles follows periodic trajectories of an incompressible (nearly) Stokes flow. The 3D isotropic porous medium instead acts as a random noise that perturbs the particle trajectories making them linearly diverging in time as a usual Brownian diffusion process.

For all the considered cases within a range $Re = 0.1 \div 1.0$, the diffusion behavior of particles in the porous medium does not depend on the Reynolds number (not shown here) indicating negligible inertial effects. In contrast, the preferential orientation of the porous medium affects the transport in the transverse direction.

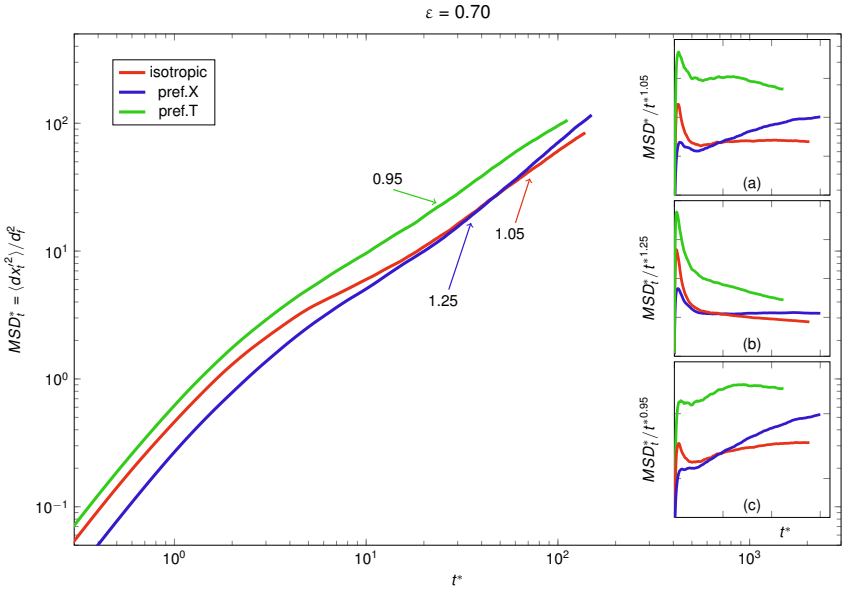

Figure 4: Non-dimensional Mean Square Displacement for three different orientation and $\varepsilon = 0.7$. Insets (a), (b) and (c): Compensated Mean Square Displacements obtained dividing MSD^* by $t^{1.05}$, $t^{1.25}$ and $t^{0.95}$, respectively.

The influence of the medium orientation on particle dispersion is shown in Figs. (3) and (4) for $\varepsilon = 0.9$ and $\varepsilon = 0.7$, respectively. The isotropic medium and the medium preferentially oriented along the transverse directions show a normal diffusion with small

differences. Note that the medium preferentially oriented along the transversal directions is now fully tridimensional cases. The mean square displacement is well represented by a standard diffusion equation, typical of Brownian processes:

$$MSD^* = 4D \cdot t^{*\alpha} \tag{5}$$

with $\alpha = 1 \pm 0.05$, see the (a) and (c) insets of Figg. (3) and (4). The diffusion coefficient D is similar in cases at same porosity. Surprisingly, when the medium is preferentially oriented along the streamwise direction, we observe and exponent $\alpha = 1.25$, that denotes once again a superdiffusive behavior ($\alpha > 1$). It is clear that for sufficiently long observation times t^* the dispersion of particle trajectories becomes significantly higher than for the other cases.

An explanation of this anomalous diffusion could be found considering the anisotropic geometry of the porous medium, in which the fibers are preferentially oriented with small angles with respect to the x axis. We believe that particles can occasionally follow the fiber surface along their axes for long distances, pushed by the pressure-gradient force. This highly correlated motion leads to high transverse displacement enhancing the diffusion process. The process could be modeled as a Levy-flight process where particles intermittently show long displacement when their trajectory is constrained for long time by almost aligned fibers.

The influence of the porosity ε on particle diffusion can be highlighted by comparing Figs. (3) and (4). While the α exponent remains the same, the diffusion coefficients are slightly higher by decreasing the porosity. Anyway the influence on particles dispersion of the diffusion coefficients (with $\alpha = 1$) is subleading compared to effect of a super-diffusive behavior with $\alpha > 1$ for long enough observation times t^*.

Table 1: Diffusion coefficients D, equivalent mass diffusion coefficients D_{eff}, effective viscosities ν_{eff} and Schmidt numbers Sc with $\varepsilon = 0.9$

case	α	D	ℓ^*	D_{eff}	ν_{eff}	Sc_{eff}
isotropic	1.05	0.09	10	0.12	0.37	3.03
isotropic	1.05	0.09	100	0.15	0.37	2.43
isotropic	1.05	0.09	1000	0.19	0.37	1.95
pref.X	1.25	0.04	10	0.14	0.29	2.03
pref.X	1.25	0.04	100	0.36	0.29	0.81
pref.X	1.25	0.04	1000	0.91	0.29	0.32
pref.T	0.95	0.18	10	0.14	0.47	3.28
pref.T	0.95	0.18	100	0.11	0.47	4.18
pref.T	0.95	0.18	1000	0.09	0.47	5.33

Table 2: Diffusion coefficients D, equivalent mass diffusion coefficients D_{eff}, effective viscosities ν_{eff} and Schmidt numbers Sc with $\varepsilon = 0.7$

case	α	D	ℓ^*	D_{eff}	ν_{eff}	Sc_{eff}
isotropic	1.05	0.12	10	0.15	3.38	21.82
isotropic	1.05	0.12	100	0.19	3.38	17.52
isotropic	1.05	0.12	1000	0.24	3.38	14.07
pref.X	1.25	0.06	10	0.19	2.27	12.12
pref.X	1.25	0.06	100	0.47	2.27	4.83
pref.X	1.25	0.06	1000	1.18	2.27	1.92
pref.T	0.95	0.30	10	0.24	4.18	17.57
pref.T	0.95	0.30	100	0.19	4.18	22.39
pref.T	0.95	0.30	1000	0.15	4.18	28.54

When dealing with diffusion of species inside porous media, it is useful to predict the mass transport via convection-diffusion-reaction Eulerian equations for the homogenized volume. When a standard diffusion process ($\alpha = 1$) takes place, the only parameter needed is the effective mass diffusion coefficient D_{eff}. Unfortunately, when $\alpha > 1$ the corresponding Eulerian transport equation is constituted by with nontrivial fractional derivatives [9]. In order to overcome this issue, it is convenient for applications to transform the super-diffusive process in a equivalent standard diffusion process in order to solve a standard convection-diffusion-reaction equation for the Eulerian homogenized mass transport. However it is necessary to to fix a typical displacement length $\ell^* \equiv \ell/d_f$ that characterizes the diffusion process of the system. The equivalent system is then obtained matching the real $MSD^* = \ell^{*2}$ with the equivalent normal diffusion process characterized by D_{eff}. The effective mass diffusivity can thus be derived by imposing the following equality:

$$\ell^{*2} = 4D \cdot t^{*\alpha} = 4D_{eff} \cdot t^* \ , \tag{6}$$

from which it follows:

$$D_{eff}(\ell^*) = 4^{\frac{1-\alpha}{\alpha}} \cdot D^{\frac{1}{\alpha}} \cdot \ell^{*2\frac{\alpha-1}{\alpha}} \ . \tag{7}$$

The Tabs. (1) and (2) report the values of D and D_{eff} for the cases $\varepsilon = 0.9$ and $\varepsilon = 0.7$, respectively, and for different characteristic displacement ℓ^*. The dispersion prediction by means of the equivalent mass diffusion coefficient D_{eff} with varying the characteristic length ℓ^* is well depicted in Fig.(5), right panel.

The medium preferentially oriented along the streamwise direction presents the higher equivalent mass diffusion coefficients, confirming the fast dispersion properties of the super-diffusive process. The effective diffusivity is higher for the lower porosity (i.e. $\varepsilon = 0.7$). However, even though the effective diffusivity is higher, also the drag exerted by the

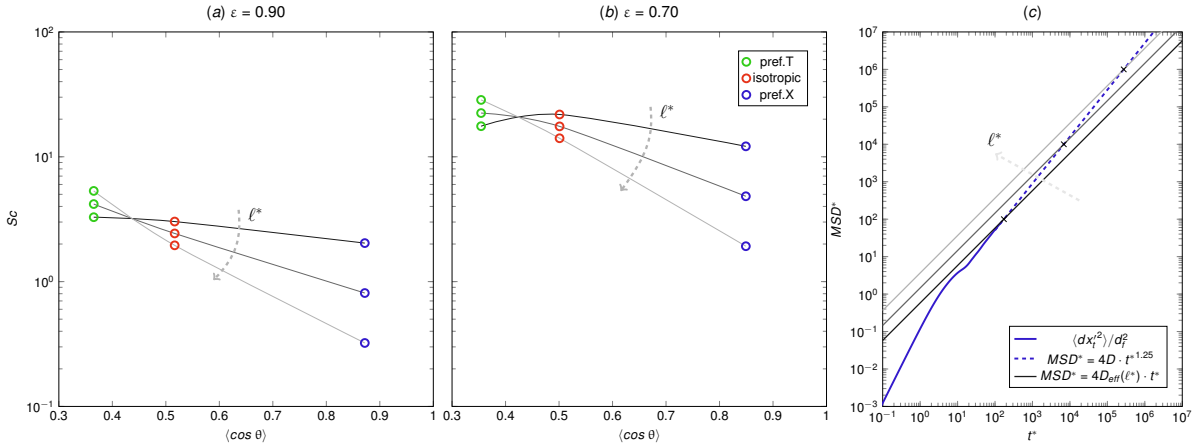

Figure 5: (a) Schmidt number plotted against the mean value of the cosine of the angle θ formed by the fibers axes and the x axis, for $\varepsilon = 0.9$, with varying the fixed characteristic lenght ℓ^*. (b) Schmidt number plotted against the mean value of the cosine of the angle θ, for $\varepsilon = 0.7$, with varying the fixed characteristic lenght ℓ^*. (c) Mean Square Displacement prediction with the normal effective coefficient D_{eff} with varying the fixed characateristic lenght ℓ^*.

fluid is higher, being higher the surface of fibers opposing the flow, see Fig.(2). In order to take into account the both mechanisms, an effective viscosity ν_{eff} has been derived as the ratio between pressure-gradient force and viscous forces:

$$\nu_{eff} = \left(\frac{DP}{Dx} \frac{1}{\rho} \right) \frac{d_f^2}{U} \ . \tag{8}$$

Following this approach, the effective Schmidt number Sc_{eff} can be obtained by combining Eq.(7) and Eq.(8):

$$Sc_{eff} = \frac{\nu_{eff}}{D_{eff}} \ . \tag{9}$$

The effective Schmidt number values are reported for all cases in Tabs. (1) and (2) and the influence of the porous medium orientation on Sc_{eff} is depicted in Fig.(5), in the left and central panel. The lower the Schimdt number, the lower the ratio between the effective viscosity and the effective diffusion. In other words, low Schmidt numbers indicate low drag and high diffusivity, which in turn increases the VRFB performances. Thus, the medium preferentially oriented along the streamwise direction and with high porosity value (i.e. $\varepsilon = 0.9$), is the best configuration for VRFBs, allowing high diffusion and low pressure losses. Fig.(5) also shows that the benefits of using an oriented medium along the streamwise direction are more significant with increasing the characteristic displacement ℓ^*. Therefore, the orientation of the medium can significantly increase the performances of VRFBs, specially when the porous medium is thick which corresponds to high typical transversal length.

4 CONCLUSION

A Lattice-Boltzmann-Method in combination with a Lagrangian Particle Tracking algorithm has been used to investigate the effects of the microscopic properties of porous media on the mass and momentum transport, i.e. mixing and drag properties. These features are crucial to optimize and increase the performance of Vanadium-Redox-Flow-Battery. The present study shows that the nematic properties of the medium, i.e. the orientation properties, crucially affect the mass dispersion process. In particular a super-diffusive behavior is observed for all the considered porous media when the mass dispersion is evaluated along the streamwise direction. On the contrary a normal diffusive behavior is observed in the transversal direction when the constituting medium fibers are either isotropically oriented or preferentially oriented along the transversal directions. Surprisingly if the constituting fibers are preferentially oriented along the streamwise direction the transversal dispersion process is super-diffusive. This greatly enhances the transversal mixing. An effective model has been proposed to characterize this behavior in standard convection-diffusion Eulerian equation determining an effective diffusion coefficient which, however, depends also on the characteristic transversal scale of the system. Finally we have shown that the porous medium with preferentially oriented fibers along the flow direction shows also the smallest drag, as expected. Hence this kind of medium appears to be the optimal solution to enhance the mixing and minimizing the pressure drop in VRFB cells.

ACKNOWLEDGEMENTS : This work was supported as part of the MAESTRA project (From Materials for Membrane-Electrode Assemblies to Electric Energy Conversion and Storage Devices, 2014 - 2016) funded by the University of Padova.

REFERENCES

[1] P. Alotto, M. Guarnieri and F. Moro. Redox flow batteries for the storage of renewable energy: A review. *Renewable and Sustainable Energy Reviews* (2014) **29**:325-335.

[2] A. Tang, J. Bao and M. Skyllas-Kazacos. Studies on pressure losses and flow rate optimization in vanadium redox flow batteries. *Journal of Power Sources* (2014) **248**:154-162.

[3] A. Z. Weber, M. M. Mench, J. P. Meyers, P. N. Ross, J. T. Gostick, Q. Liu. Redox flow batteries: a review. *Journal of Applied Electrochemistry* (2011) **41**(10):1137-1164.

[4] S. Whitaker. The Forchheimer Equation: A Theoretical Development. *Transport in Porous Media* (1996) **25**:26-61.

[5] P. K. Kang, P. de Anna, J. P. Nunes, B. Bijeljic, M. J. Blunt and R. Juanes. Pore-scale intermittent velocity structure underpinning anomalous transport through 3-D porous media. *Geophysical Research Letters* (2014) **41**:6184-6190.

[6] S. Succi. *The Lattice Boltzmann Equation: for Fluid Dynamics and Beyond*. Oxford University Press (2001).

[7] D. Maggiolo, A. Marion, and M. Guarnieri. Lattice Boltzmann Modeling of Water Cumulation at the Gas Channel-Gas Diffusion Layer Interface in Polymer Electrolyte Membrane Fuel Cells. *Journal of Fuel Cell Science and Technology* (2014) 11(6):061008.

[8] D. d'Humieres, I. Ginzburg, M. Krafczyk, P. Lallemand and L. S. Luo. Multiple-relaxation-time lattice Boltzmann models in three dimensions. *Philosophical Transanction of the Royal Society of London A* (2002) **360**:437-451.

[9] D. Brockmann. *Superdiffusion in Scale-Free Inhomogeneous Environments*. Dissertation at Georg-August-University Gottingen (2003).